Biophysical Journal, Volume *115*

Supplemental Information

Light-Activated Dynamic Clamp Using iPSC-Derived Cardiomyocytes

Bonnie Quach, Trine Krogh-Madsen, Emilia Entcheva, and David J. Christini

SUPPORTING MATERIAL

for

Optical dynamic clamp using iPSC-derived cardiomyocytes

by

Bonnie Quach, Trine Krogh-Madsen, Emilia Entcheva, and David J. Christini

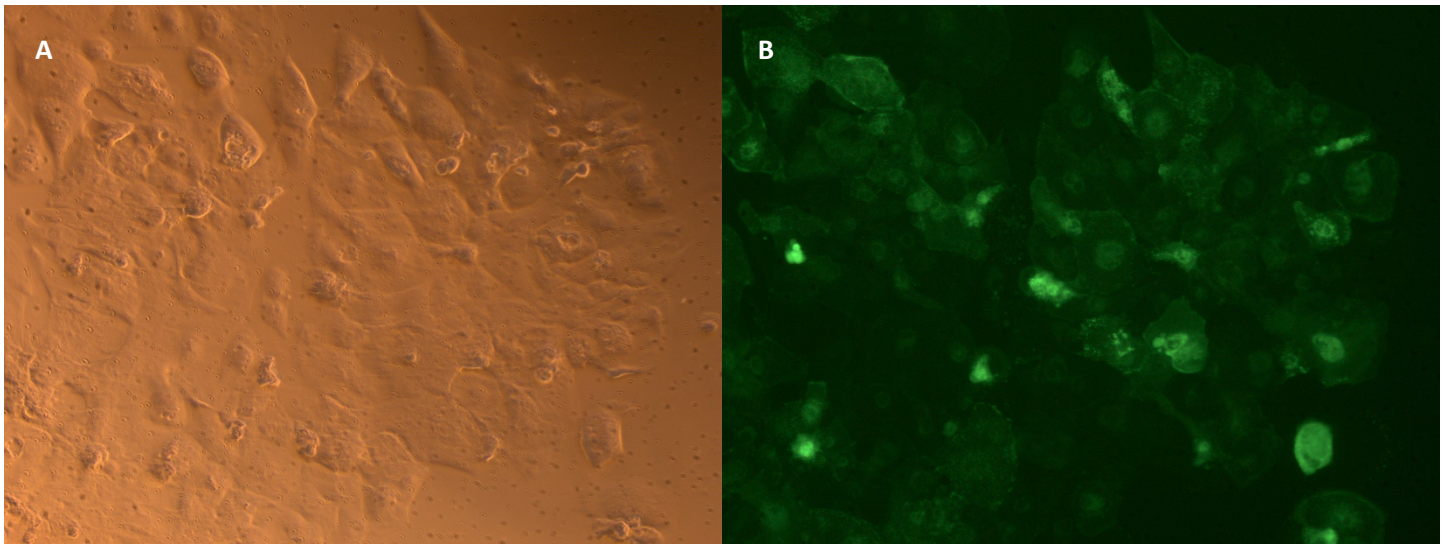

Figure S1: Successful ArchT-eGFP expression in iPSC-CMs

Visualization of eGFP expression following the transfection protocol by Ambrosi and Entcheva (2014).

A) Brightfield image of iPSC-CM beating clusters at 40x.

B) Corresponding image of eGFP fluorescence at 40x.

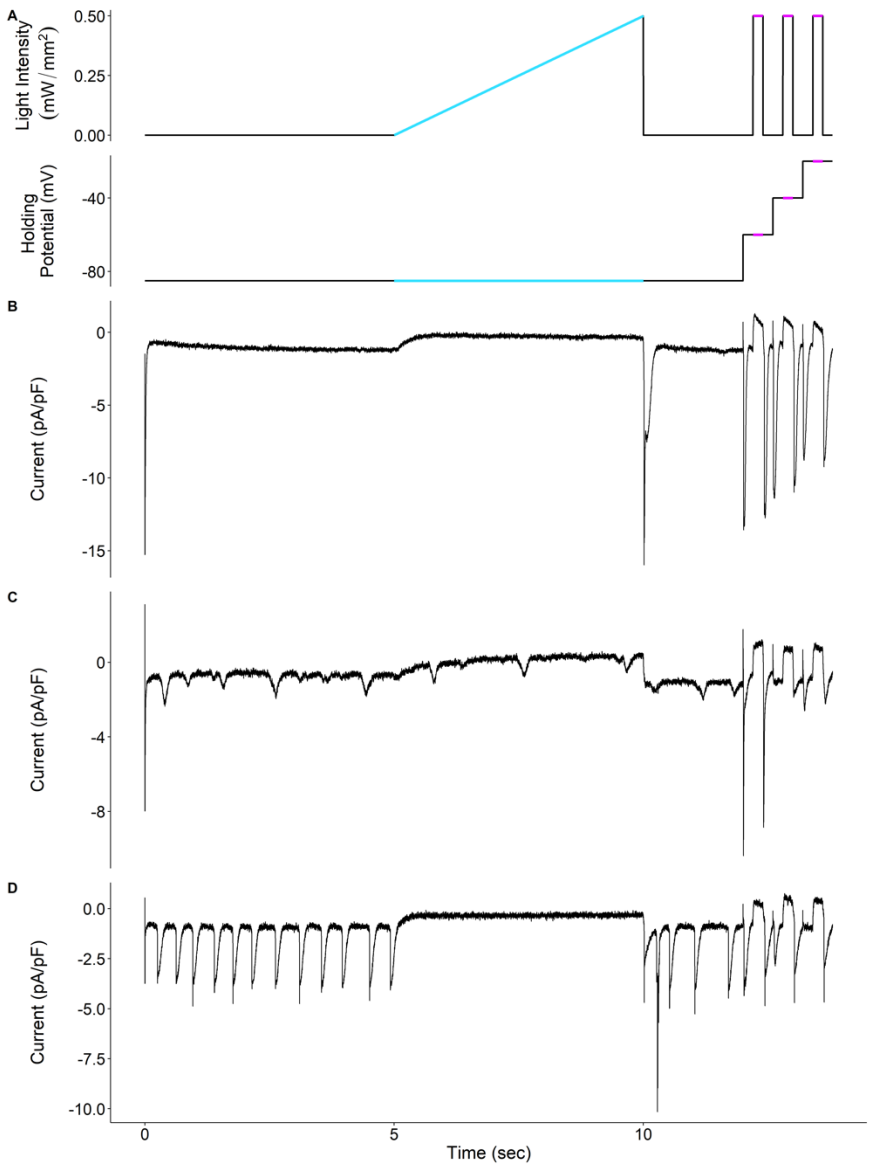

Figure S2: Representative examples of calibration protocol outputs

The calibration protocol (A) can yield a variety of current outputs (B-D) that may be interrupted by repetitive large inward currents (C, D). These inward currents are associated with spontaneous contractions (C, D) which in some cases are suppressed with ArchT activation (D).

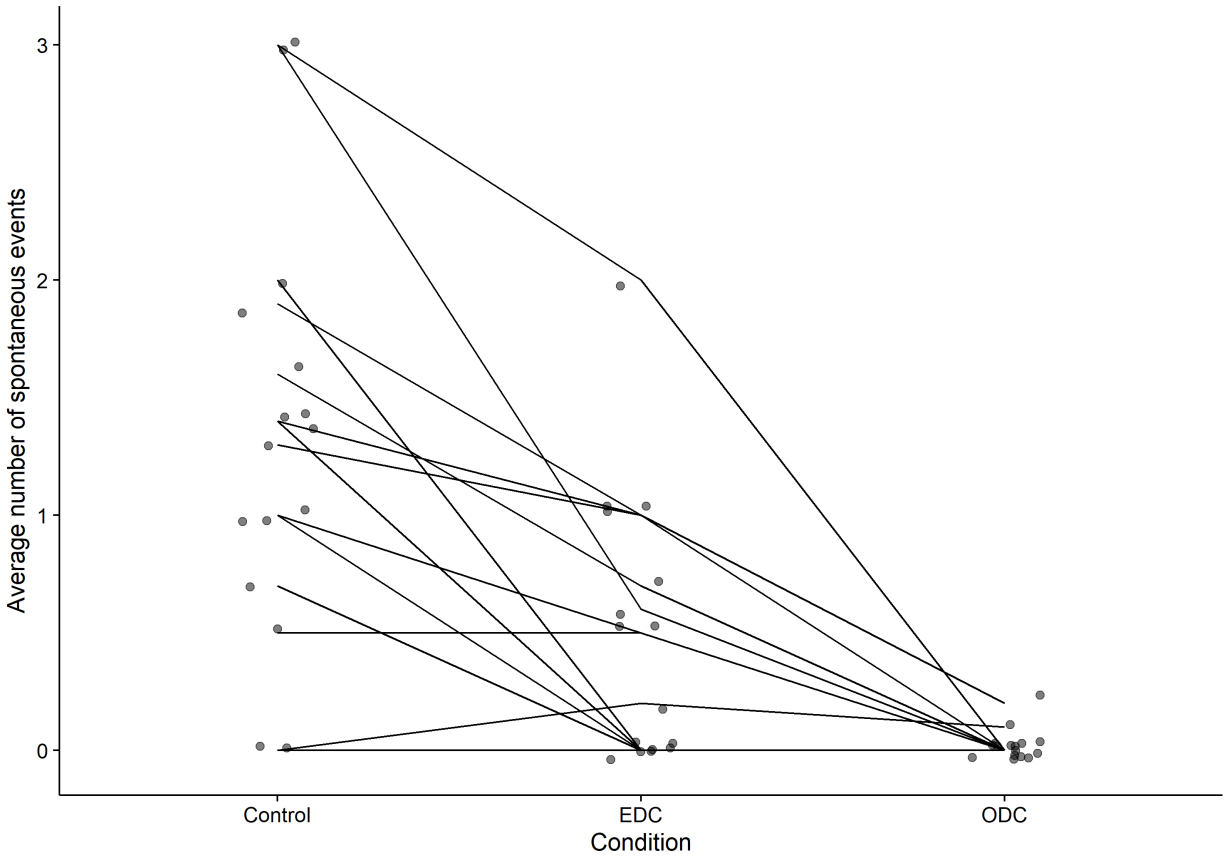

Figure S3: Decrease in spontaneous activity with ODC.

Average number of spontaneous events occurring during sequence of 10 stimulated APs at 0.5 Hz pacing. Each point represents a different cell and the lines connect the results from the same cell.

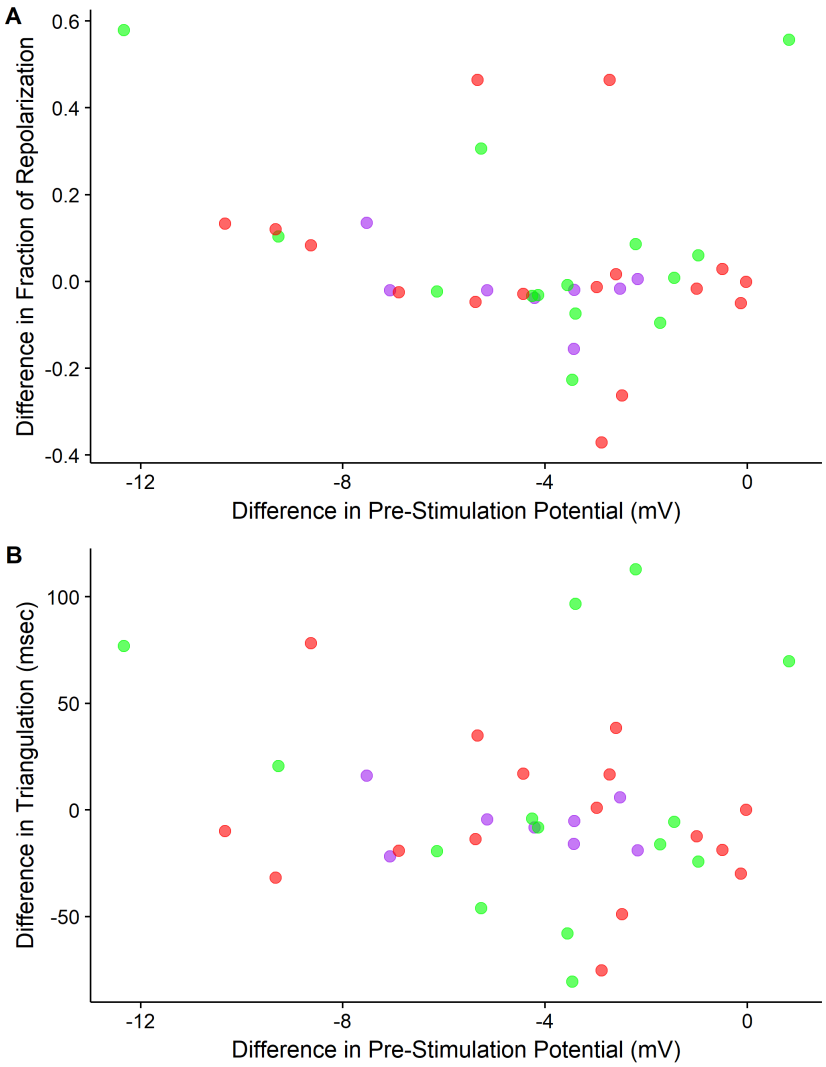

Figure S4: Difference in pre-stimulation potential between EDC and ODC does not correlate with differences in AP morphology characteristics between EDC and ODC

(A) Difference in pre-stimulation potential on difference in fraction of repolarization time. Results at 0.5 Hz, 1 Hz and 2Hz pacing are purple, green, and red, respectively.

(B) Difference in pre-stimulation potential on difference in triangulation. Results at 0.5 Hz, 1 Hz and 2Hz pacing are purple, green, and red, respectively.

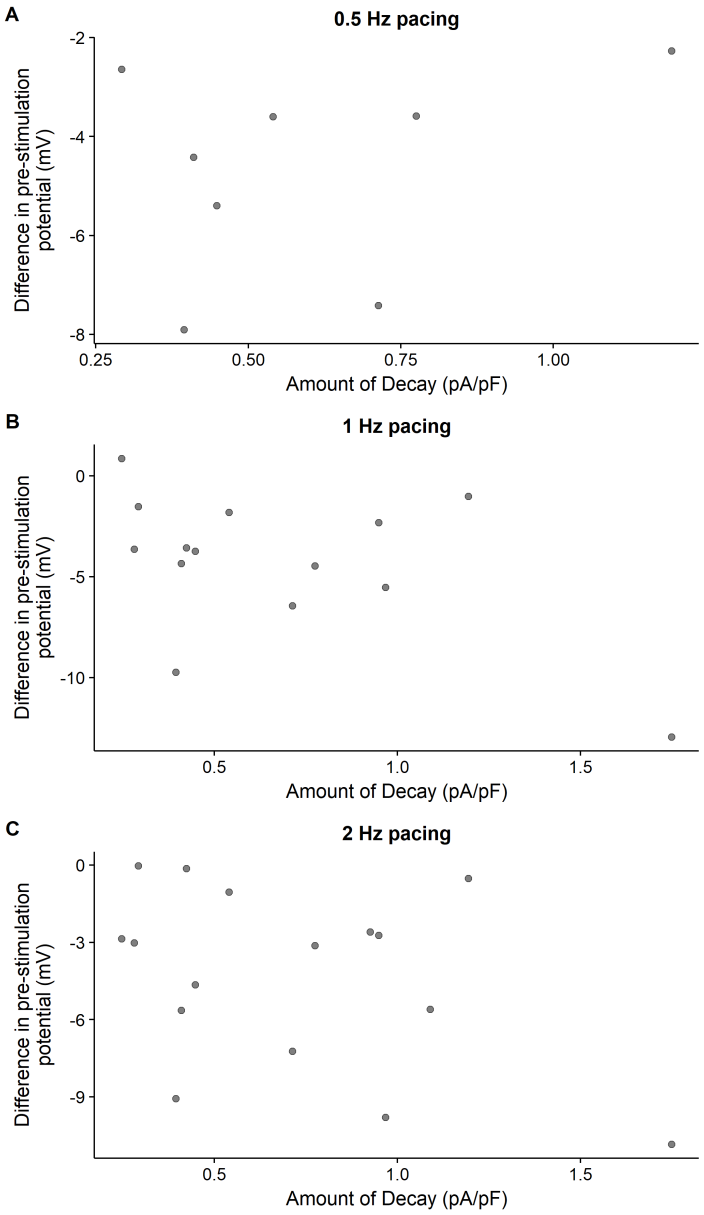

Figure S5: Amount of current decay during constant-intensity light pulses does not correlate with the difference in pre-stimulation potential between EDC and ODC

The amount of current decay was measured as an average difference between the initial current and the final current during the three constant-intensity (0.5 mW/mm^2) light pulses during the calibration protocol. The amount of current decay was compared to the average difference in pre-stimulation potential (mV) between EDC and ODC at (A) 0.5 Hz, (B) 1 Hz, and (C) 2 Hz. Each point represents a different cell.

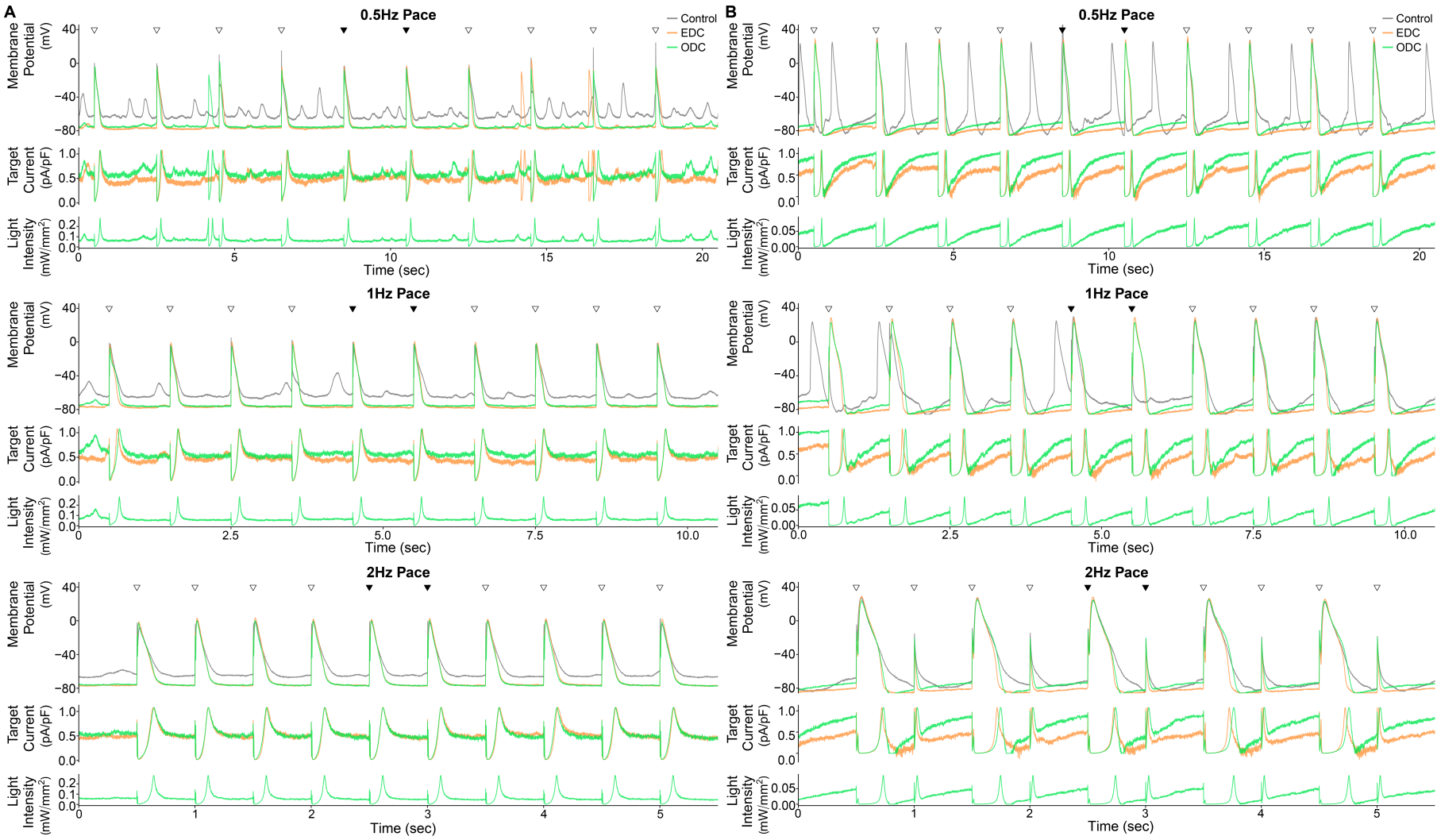
A
B
0.5Hz Pace
1Hz Pace
2Hz Pace
Control
EDC
ODC
Membrane Potential (mV)
Target Current (pA/pF)
Light Intensity (mW/mm²)
Time (sec)

Figure S6: Entire trace of 10 paced APs demonstrating the results of the EDC and ODC platforms from example cells

Results from example cell 1 (A) and cell 10 (B) showing the effects of adding I_{K1} while paced 10 times at 3 different frequencies: 0.5 Hz (top), 1 Hz (middle), 2Hz (bottom). The gray, orange and green traces represent the control without any current addition, adding I_{target} with EDC, and adding I_{target} with ODC, respectively. For each pacing rate, the top panel overlays the 10 paced AP traces over time under control and both dynamic-clamp conditions, and the black triangles indicate when a stimulus current was delivered. In the middle panel, the traces give the calculated target currents for EDC and ODC. The bottom panel shows the calculated light intensity used to generate the target current. The filled black triangles indicate when a stimulus current was delivered and provides a reference to which of the 10 paced APs in Figures 3 (A) and 4 (B) are displayed.

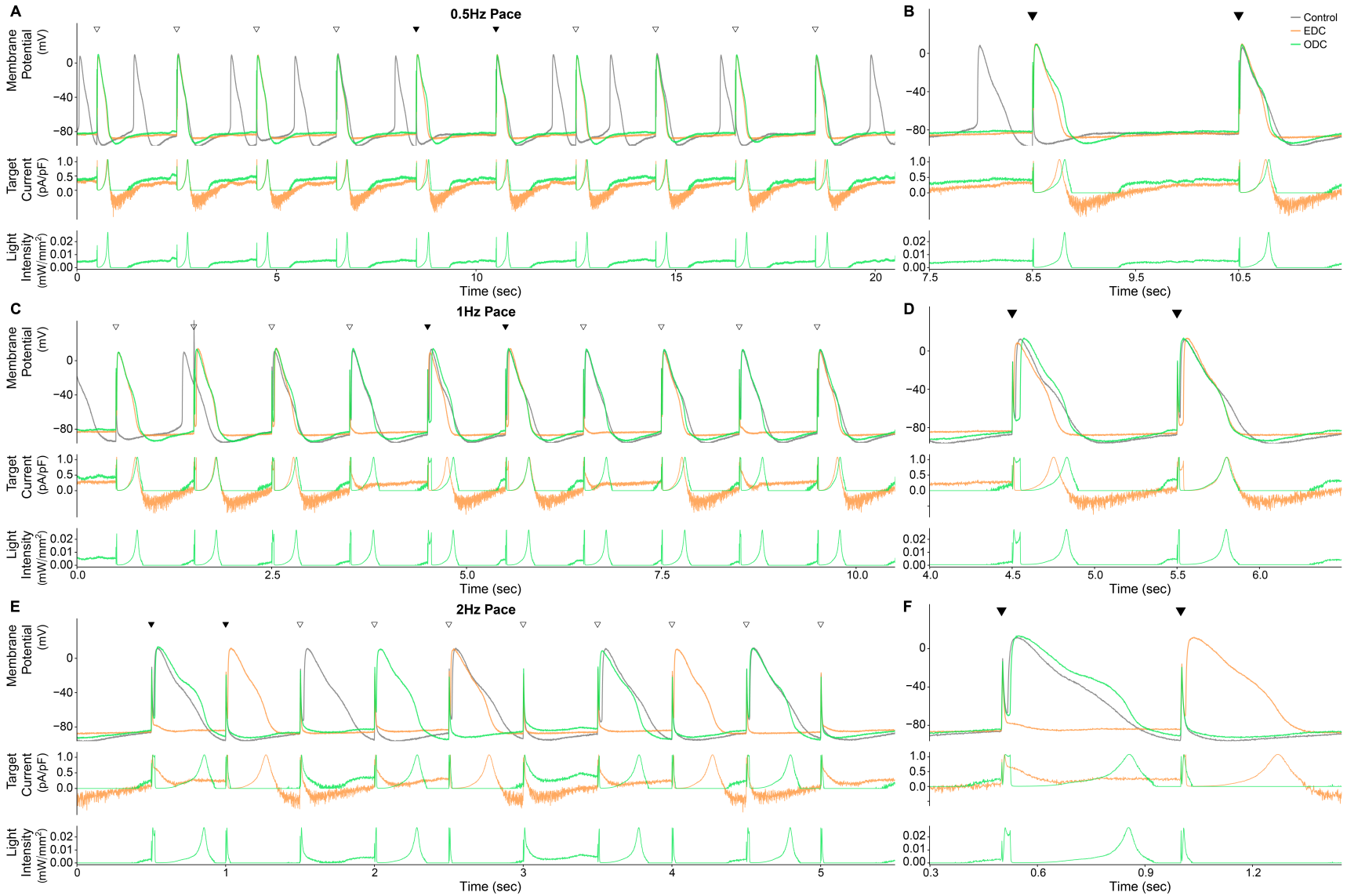
A
0.5Hz Pace
B
Control
EDC
ODC
C
1Hz Pace
D
E
2Hz Pace
F
Membrane Potential (mV)
Target Current (pA/pF)
Light Intensity (mW/mm²)
Time (sec)

Figure S7: Representative example of a large undershoot after an AP and how EDC is able to compensate for the undershoot

Example cell (cell 3) showing the effects of adding I_{K1} while paced 10 times at 3 different frequencies: (A, B) 0.5 Hz, (C, D) 1 Hz, (E, F) 2Hz. The gray, orange and green traces represent the control without any current addition, adding I_{target} with EDC, and adding I_{target} with ODC, respectively. The top panels overlay the 10 paced AP traces under control and both dynamic-clamp conditions, and the black triangles indicate when a stimulus current was delivered. In the middle panels, the traces give the calculated target currents for EDC and ODC. The bottom panels show the calculated light intensity used to generate the target current with ODC. The filled black triangles in the top panels (A, C, E) provide a reference for zoomed portions shown in B, D, and F, respectively.

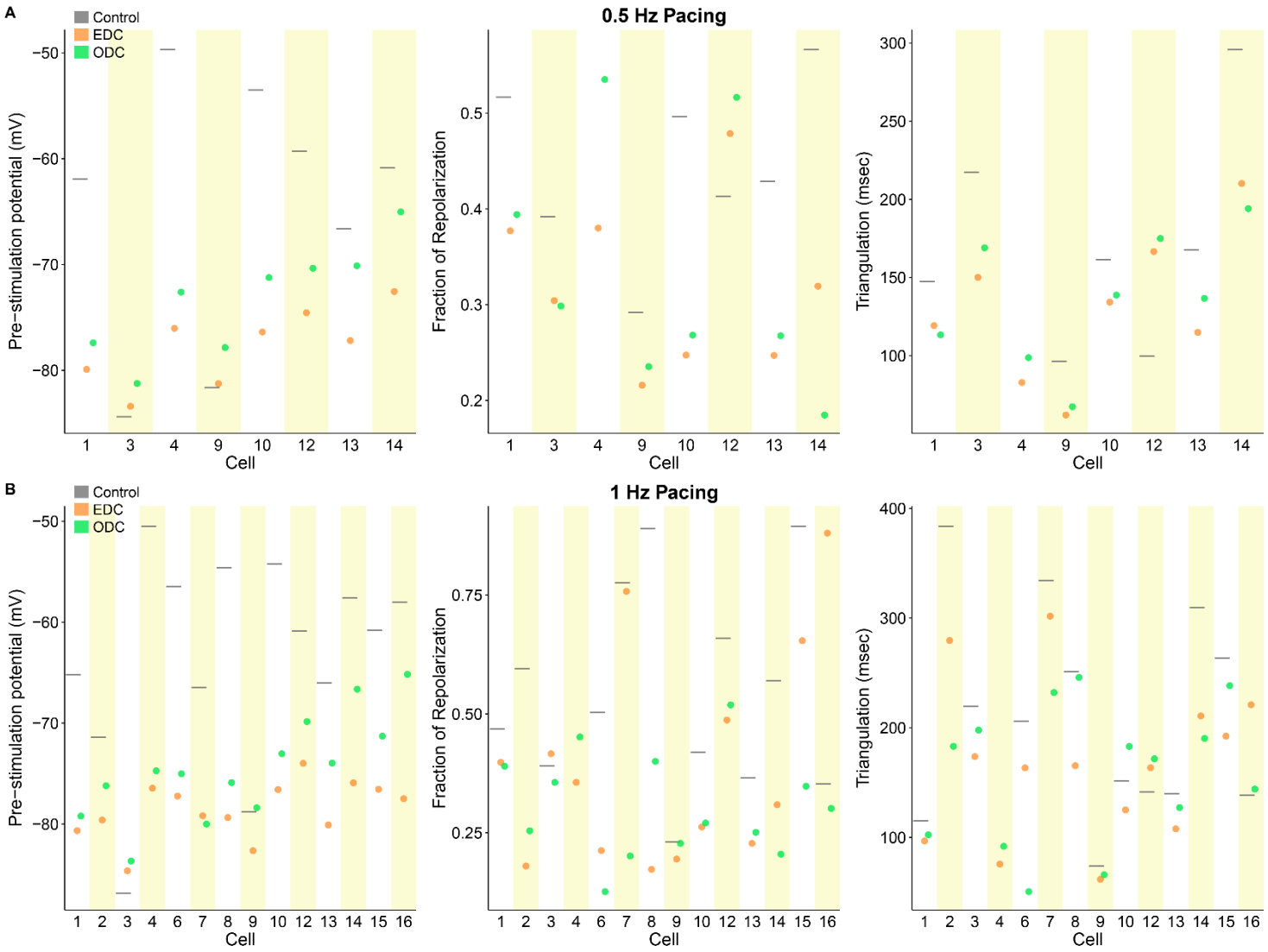

Figure S8: Summary of the effects of EDC or ODC on AP morphology at different pacing frequencies

Pre-stimulation potential (left), fraction of repolarization (middle) and triangulation (right) of individual cells at 0.5 Hz (A) and 1 Hz (B) pacing in control (gray) and after adding an I_{K1} target current via EDC (orange) or ODC (green).

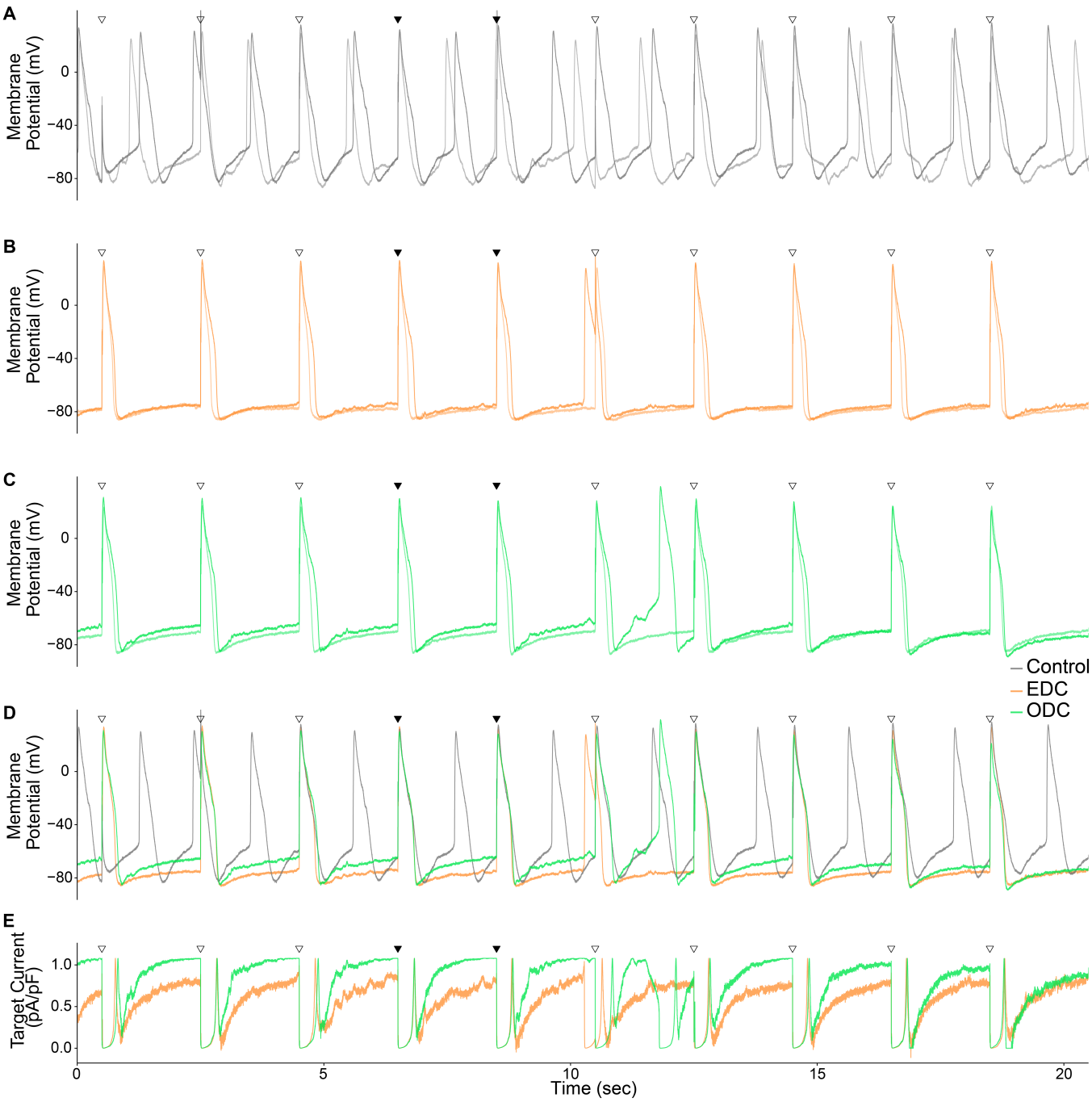

Figure S9: Entire trace of 10 paced APs demonstrating the results of the EDC and ODC platforms from example cell with E-4031 addition

Results from example cell 13 showing the effects of adding I_{K1} while paced 10 times at 0.5 Hz. The figure is organized in the same manner as Figure S6.

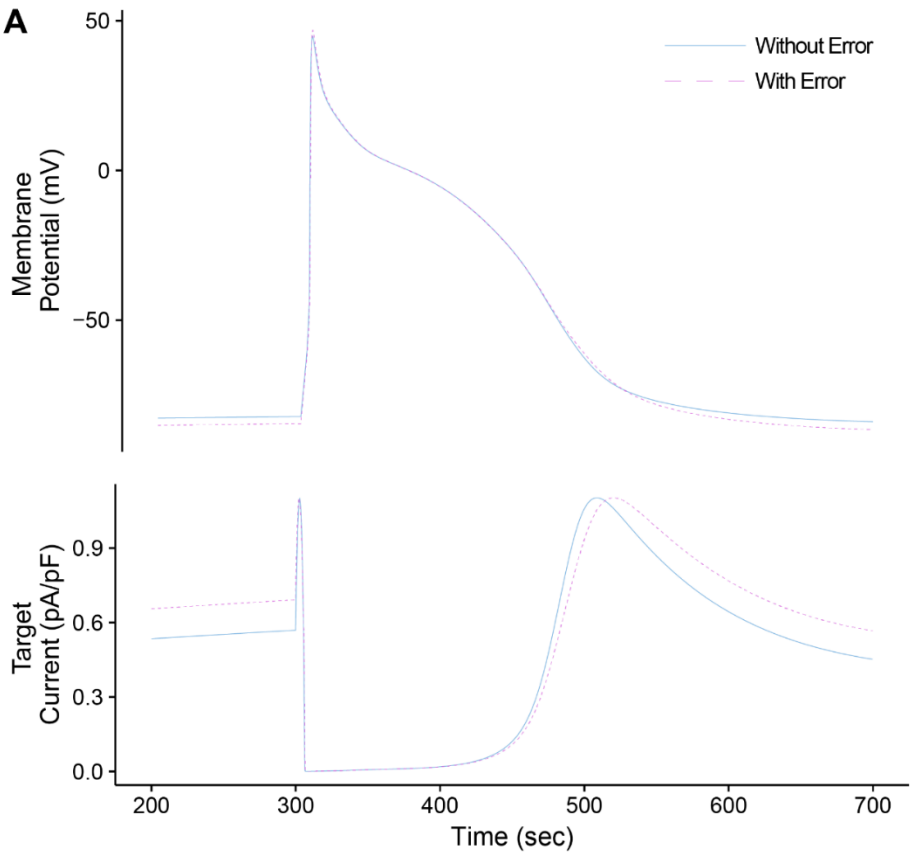

B

	Without Error	With Error
Pre−Stimulation Potential (mV)	−82.4	−84.7
APD_{90} (msec)	214.4	221.9

Figure S10: *In silico* model prediction shows that the error between RTXI and the amplifier has limited impact on dynamic clamp experiments

To predict the effects on dynamic clamp performance of the 5% error between the membrane potential measured by the amplifier versus the membrane potential reported by RTXI, we used an *in silico* approach, simulating I_{K1} dynamic clamp injection into an iPSC-CM computational model (Paci et al., (2013)). We used the same equations for I_{K1} as in our experiments and clamped intracellular $[Na^+]$ to mimic a patched cell. The dynamically clamped iPSC-CM model was run for 810 beats at a 1 Hz pacing rate with and without the amplifier calibration error and the last 10 APs were analyzed. (A) The top panel illustrates the last AP waveform with (dashed purple trace) and without (blue trace) the error. The

bottom panel shows the corresponding target I_{K1}. The presence of the calibration error leads to an overestimation of this current during phase 4 of the AP, causing a small (about 2 mV) hyperpolarization of the resting membrane potential. (B) The resulting AP characteristics with and without the calibration error are very close, with about a 3% change in APD_{90}. Importantly, the predicted effect of the calibration error calculated here does not depend on how the dynamic clamp target current is added to the cell and is therefore expected to affect I_{target} calculated by the EDC and ODC systems equally.

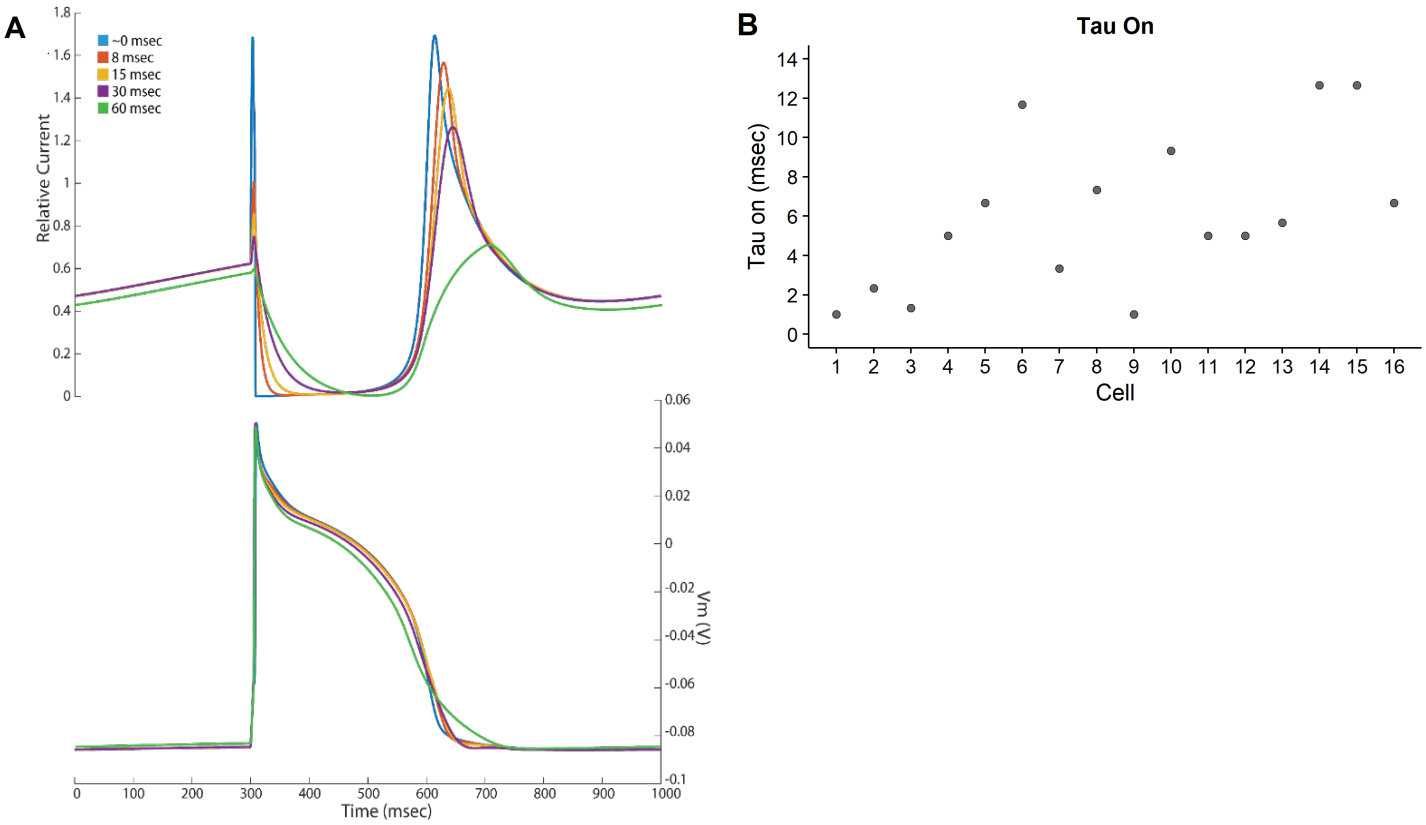

Figure S11: *In silico* model predicting the effect of activation and deactivation kinetics on dynamic clamp performance and experimentally measured ArchT time constants

(A) To test that the kinetics of ArchT are not prohibitively slow for dynamic clamp, we simulated our ODC platform using the Paci et al. (2013) iPSC-CM model with an added ArchT model having a single time constant for activation and deactivation. We varied this time constant to see how large of a delay could be tolerated. The ArchT current generated with different time constants are displayed in the panel above and sthe resulting stimulated APs are in the panel below.

(B) Experimentally measured time constants of activation of ArchT in each cell.

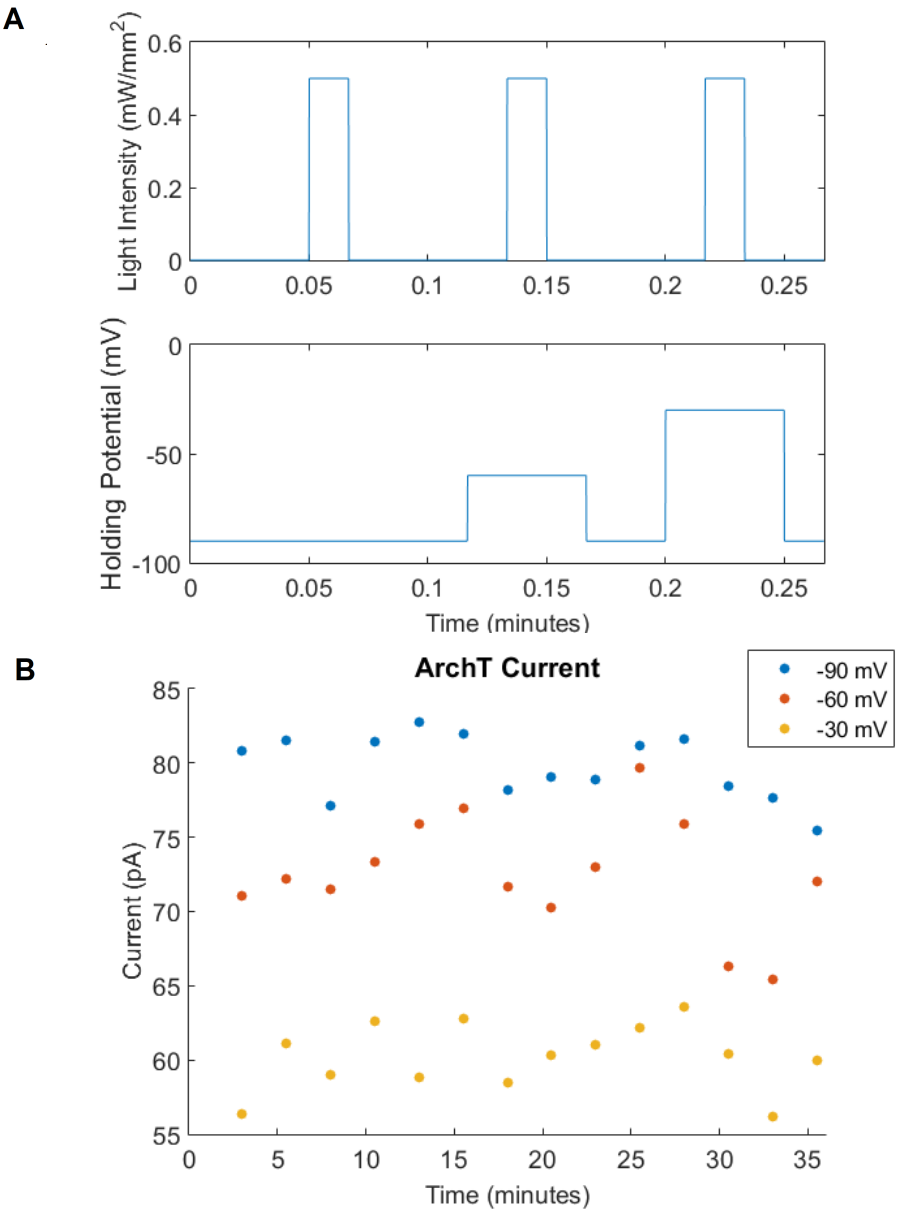

Figure S12: Measuring stability of ArchT illumination during a voltage clamp and light clamp protocol

(A) The top panel shows the light clamp protocol and the bottom panel shows the voltage clamp protocol. This protocol was cycled through repeatedly to measure I_{ArchT} over time and at different holding potentials

(B) Results from a representative cell showing I_{ArchT} produced at different times of the protocol and at different holding potentials.

	PSP			Overshoot			APD_{90}		
	Control	EDC	ODC	Control	EDC	ODC	Control	EDC	ODC
2Hz	-64.9 ± 2.5	-78.3 ± 0.7	-74.2 ± 1.3	22.5 ± 2.9	21.5 ± 2.4	15.4 ± 2.3	265.3 ± 17.7	251.8 ± 17.5	267.0 ± 18.5
1 Hz	-63.2 ± 2.7	-78.6 ± 0.8	-74.5 ± 1.4	21.6 ± 3.4	21.1 ± 5.6	14.6 ± 2.5	269.9 ± 22.4	259.6 ± 20.7	261.7 ± 19.9
0.5 Hz	-64.6 ± 4.4	-77.7 ± 1.3	-73.2 ± 1.9	18.3 ± 4.9	14.8 ± 5.2	11.6 ± 3.8	254.1 ± 30.1	235.2 ± 24.9	241.0 ± 28.1
E4031	-64.1 ± 4.6	-75.8 ± 1.4	-71.1 ± 2.3	7.8 ± 7.3	16.7 ± 6.3	16.4 ± 5.3	711.6 ± 215.8	448.2 ± 98.3	483.6 ± 103.1

Table S1: AP morphology characteristics

The average and SEM of pre-stimulation potential (PSP) (mV), overshoot (mV), and APD_{90} (msec) without dynamic clamp, with EDC and with ODC. The characteristics after E-4031 addition are also listed.